Efficacy of Diffraction Imaging for identification of faults and fractures: A case study with (a) Full azimuth 3D land data and (b) Narrow azimuth 3D marine data

Abhinandan Ghosh[1], Debkumar Chatterjee, Anand Prakash, Subhankar Basu
[1]Email: ghosh_a1@ongc.co.in, Oil and Natural Gas Corporation Limited

Keywords

Wave-field decomposition, full azimuth directional angle gather, specular filter, diffraction volume, automatic fault interpretation, seismic attributes.

Abstract

This paper presents a method for maximizing fault information from depth migrated narrow azimuth as well as full azimuth seismic data. The faults are imaged in the depth domain by separating the diffracted component from the total migrated wave-field. This study demonstrates that depth domain diffraction imaging can be used to generate higher resolution fault definition than conventional reflectivity volumes, or their derivative post-stack attributes.

Introduction

Fault and fractures play key role in generating effective porosity for hydrocarbon traps in volcanic reservoir. Detailed understanding of the fault and fracture network in reservoirs is of great importance for maximizing hydrocarbon productivity and recovery efficiency. Detection and characterization of fault and fractures enable reservoir compartmentalization risk to be better quantified and can aid in the positioning of wells.

Often it is difficult to map subtle faults and other trace to trace discontinuities hidden in 3D seismic data. They may appear as minor changes in the seismic waveform that are not easily discernible using conventional interpretation of seismic cross-sections. Various seismic attributes such as coherency, curvature etc that are derived from reflection seismic data (continuity volume) have been used for more than a decade to detect fault and fractures (Chopra, Marfurt 2018). In advanced seismic fracture detection technology, automatic fault extraction (AFE) from diffraction seismic data (discontinuity volume) more effectively detects finer scale features in seismic data (Ghosh, 2019). In this study, we demonstrate the utility of this methodology with an application to:

(a) Full azimuth 3D Land seismic data from the Field A, South Cambay Basin, India and
(b) Narrow azimuth 3D Marine towed streamer seismic data from the Field B, Western Offshore Basin, India.

Theory / Methodology

“Diffraction Imaging” aims to attenuate the reflection energy, leaving behind any focused diffraction events generated by faults, unconformities and depositional discontinuities. The ability to decompose the specular and diffraction energy from the total scattered field contained within a full-azimuth directional gather is the core component of the diffraction imaging system (Koren,Z., Ravve,I., 2011). Specular energy is focused within a narrow range of specular dips, whereas diffraction energy will populate all non-specular dips (Benfield,N.R., Guise,A., Chase,D., 2016). Specular energy has higher amplitude than the diffraction energy, but the proportion of diffraction energy will increase at geological discontinuities. Thus a suitable filter can be designed to attenuate the higher amplitude specular reflections from the migrated pre-stack depth domain data. Attenuation of the specular energy leaves behind low amplitude diffraction energy only, that can be stacked to enhance any spatially consistent geological discontinuities.

To aid interpretation of the features derived from the diffraction volume, a dip-guided edge detection filter was used to considerably enhance the faults and reduce the background noise. Any incoherent events left in the diffraction volume have to be attenuated before the lineation can be automatically picked as fault. Thus a linear noise filter is optimally designed to reduce vertical or horizontal striping appeared in diffraction volume due to artifact of processing and/or acquisition. Automatic fault extraction algorithm generally picks up every lineation, generating more faults that can be practically handled. Therefore, filtering of the picking based on size, dip, azimuth and picking threshold is applied to finalize the final interpretable fault/fracture volume, keeping in mind the regional stress regime and tectonic setting of the area. The flowchart of the adopted methodology is shown below in Figure 1.

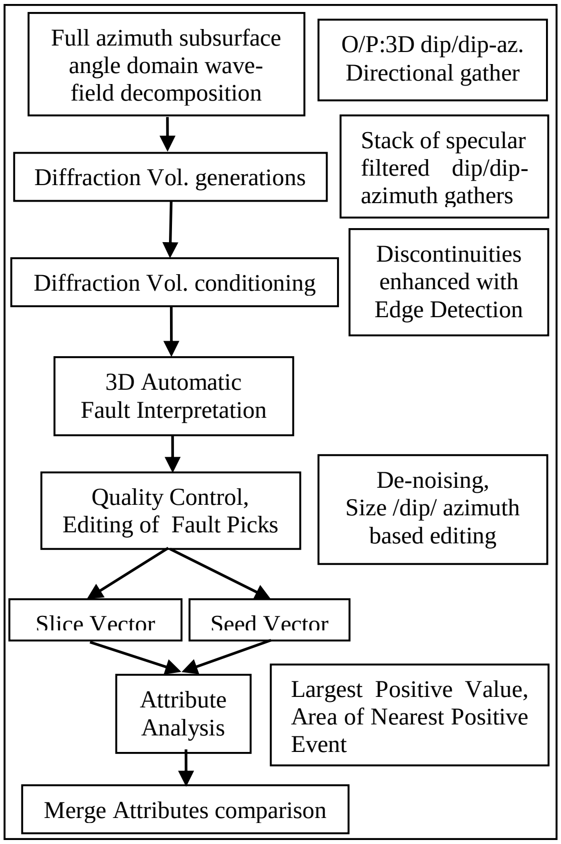

Figure 1: Diffraction Imaging to Fault Interpretation work flow.

Examples

In this study, we are experimenting with seismic data sets from two different basins of India. First one is the full azimuth 3D land data from the Field A, South Cambay Basin, India where the basaltic Deccan Trap forms the basement. Hydrocarbons are produced both from the volcanic basement fractures and from the overlaying tertiary sedimentary section viz. the Ankleshwar formation. Second one is the narrow azimuth broadband 3D marine towed streamer acquisition with 10X6km cables, towed perpendicular to the main fault trends of the hydrocarbon Field B, Western Offshore Basin, India. In this field, pay zones are Mukta, Bassein, Panna Formations, with the Ratnagiri Formation of Miocene age holding additional interest. Though commercial presence of hydrocarbon had long been established in Archean basement of Western offshore basin, focus on characterization of basement reservoir in Field B has gained prime attention very recently. Consequently, exploratory location with basement as primary objective is now being considered with equal interest.

(a) Full azimuth 3D Land data example :

The diffraction volume, generated after muting specular energy at a specified angular aperture shows enhanced imaging of spatially consistent geological discontinuities and higher resolution fault definition. The diffraction depth slice (Figure 2) shows sharp definition of intra-trap fault patterns. Sub-parallel NNW-SSE trending regional normal faults are clearly visible. Distinct differences in fault pattern across the intersection of the depth slice with the trap top (shown by green line) are clearly observed.

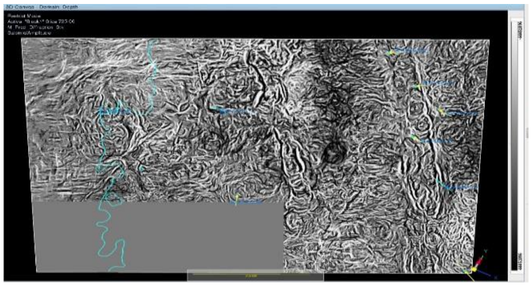

Ant Track depth slice derived from conventional

Figure 2: Diffraction Depth Slice (725m) with trap top (green line)

reflection seismic (Figure 3) and diffraction seismic (Figure 4) is shown for comparison. Clearly, fault and fracture patterns can be derived in a more reliable and geologically meaningful way using the diffraction (discontinuity) data than the conventional reflection (continuity) data.

Figure 3: Ant Track Depth Slice (725m) from Reflection Seismic

Figure 4: Ant Track Depth Slice (725m) from Diffraction Seismic

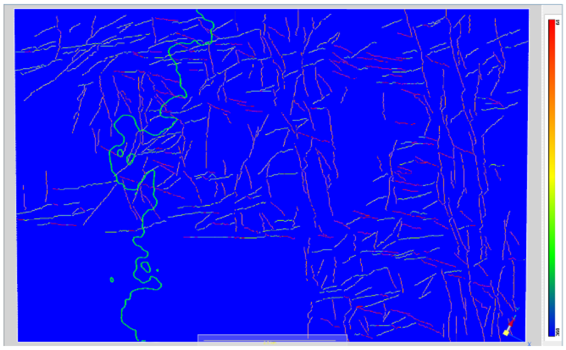

Figure 5: AFE Depth Slice (725m) from Diffraction Seismic

Finally, after application of AFE, faults have been separated from other discontinuity features present in the diffraction volume and enhanced linear and planar fault-related features are sharply defined (Figure 5). AFE analysis of diffraction volume yielded a basement fracture network that has been validated with fracture data derived from available FMI logs in the area. Fault surfaces are shown superimposed on Specular-Diffraction seismic (Figure 6).

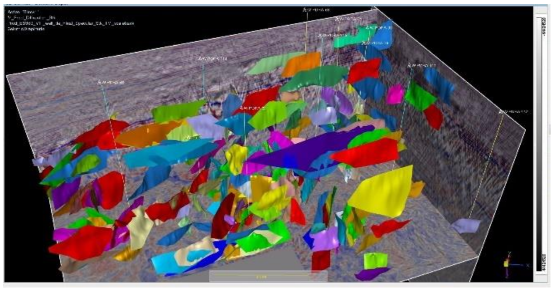

Figure 6: Fault surfaces superimposed on Specular-Diffraction Seismic

(b) Narrow azimuth 3D Marine data example: Two locations (#A & #B) at basement highs and ridges in Field B are located in vicinity the axial trend of migration pathways. Established hydrocarbon generative depression i.e. Vijaydurg graben is located in near vicinity with thick and mature source sequence, and expected to cater to the hydrocarbon charging in the area. Continuity volume co-rendered with discontinuity volume (Figure 7) with flat H1A horizon

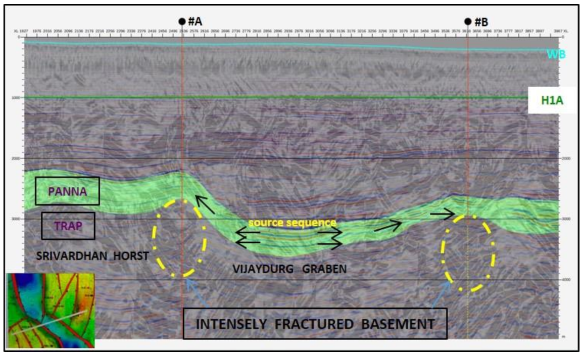

Figure 7: Seismo-geological section with flat H1A horizon.

shows both source sequence in Panna formation in Vijaydurg graben and intensely fractured basement at both well locations. Though data is from narrow azimuth marine streamer acquisition, 3D dip/dip-azimuth direction gather at target depth of both well #A (Left panel of Figure 8) and #B (Right panel of Figure 8) shows full 360° coverage, establishing the justification of diffraction imaging.

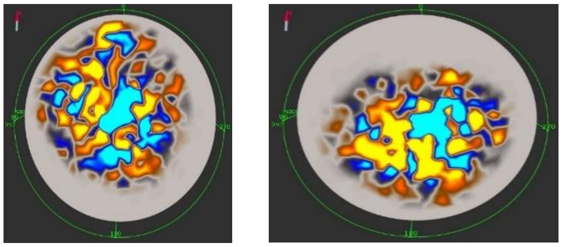

Figure 8: Target Depth Slice 3D Direction Gather at well #A (left) and well #B (right).

Diffraction volume (Figure 9) and its derivative Fault enhanced Slice vector (Figure 10) along Trap Top shows clearly NW-SE regional fault and ENE-WSW cross trends. Well #A is placed close to the intersection of two fault trends having good density of fractures. Good fracture density is also observed in well location #B in comparison to its alternate location #B*. Good connectivity of fractures in axial trend to the low towards rift shoulder is ideal for migration of hydrocarbon to fractured basement.

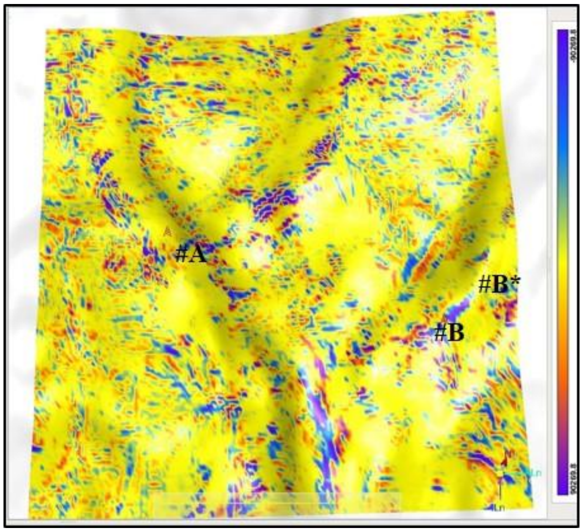

Figure 9: Diffraction volume along Trap Top

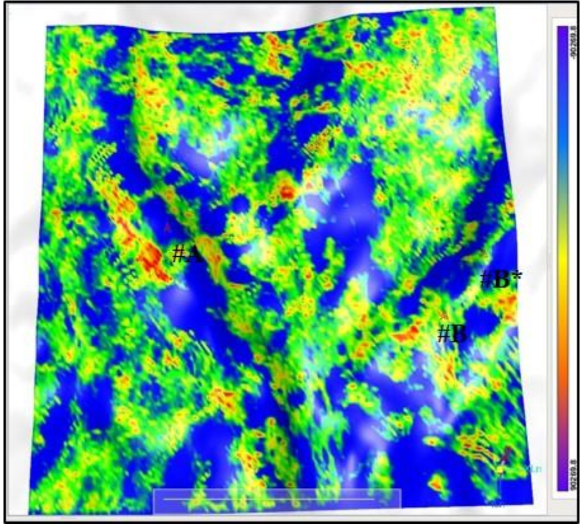

Figure 10: Fault enhanced Slice Vector along Trap Top

The lineation from the diffraction volume can be correlated directly with breaks in the reflectivity volume amplitude (Figure 7). Fault enhanced slice vector is co-rendered with specular volume to ascertain that the lineation can be attributed to faults and not just noise. The co-rendered volume at target depth of well #A (Figure 11) and well #B (Figure 12) show very good amount of fracture density.

Vintage Ant Track volume derived from conventionally processed reflection (continuity) volume can be compared at target depth of well #A (Figure 13) and well #B (Figure 14).

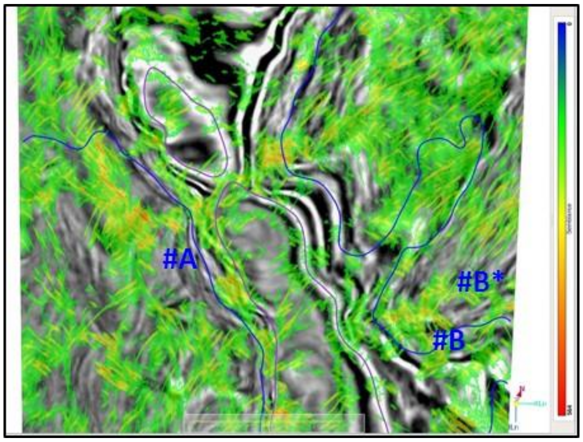

Figure 11: Specular volume (in grey-shades) co-rendered with Slice Vector (in color) at Target Depth of #A

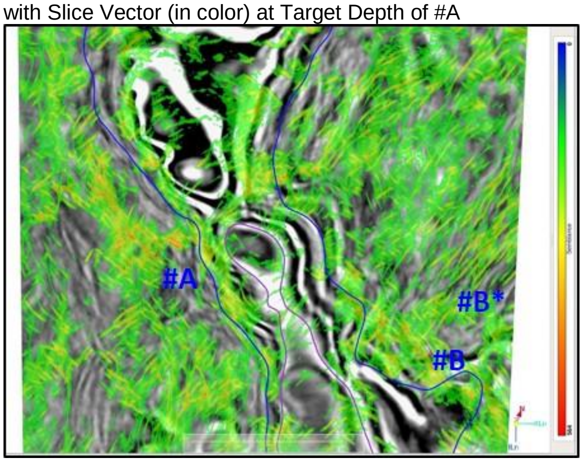

Figure 12: Specular volume (in grey-shades) co-rendered with Slice Vector (in color) at Target Depth of #B

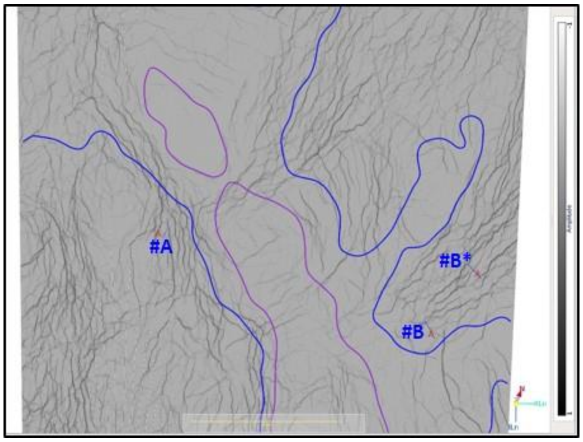

Figure 13: Vintage Ant Track volume at Target Depth of well #A.

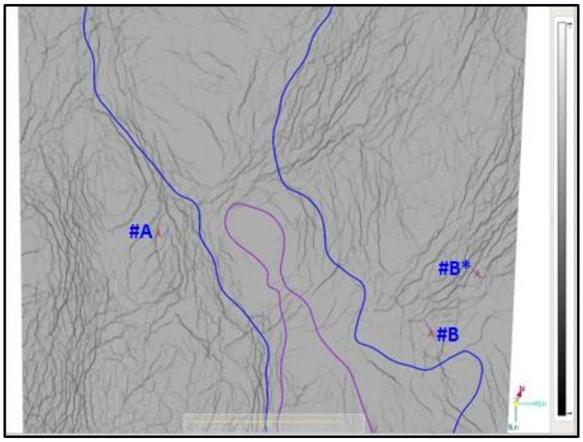

Figure 14: Vintage Ant Track volume at Target Depth of well #B

Again from Fracture Seed vector azimuth depth slice at target depth of well #A (Figure 15 left) and well #B (Figure 15 right), fracture orientation can be ascertained very clearly, which helps to determine the directivity of the inclined well.

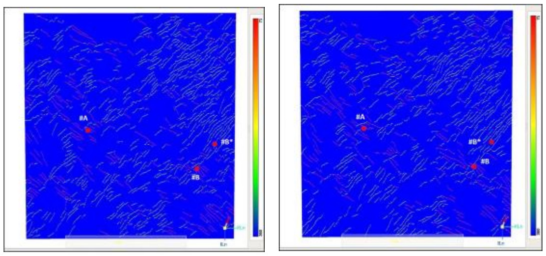

Figure 15: Seed Vector Azimuth at TD of #A (left) #B (right).

Using seed vector azimuth volume, vector azimuth rose diagram can be generated at any depth surrounding the well location (Figure 16), giving a valuable information of depth-wise localized major fracture orientation.

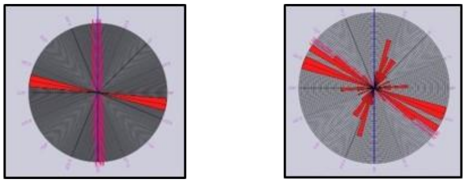

Figure 16: Seed Vector Azimuth Rose Diagram surrounding (~0.8 SKM) the well at Target Depth of #A (left) and #B (right).

Attribute analysis (Figure17-19) is studied on AFE outputs. Largest Positive Value is extracted from AFE Slice Vector and Area of Nearest Positive Event is extracted from AFE Seed Vector. Both are also extracted from vintage Ant-Track volume. Extraction window is from Trap Top to well target depth. Merge attributes of the above two are also derived.

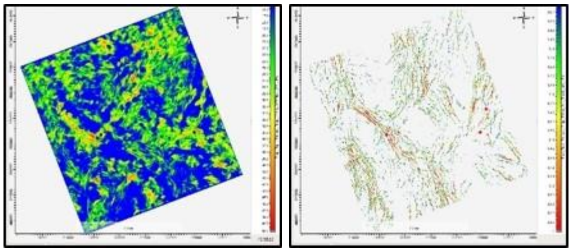

Figure 17: Largest Positive Value: Slice Vector (left), Ant-track (right).

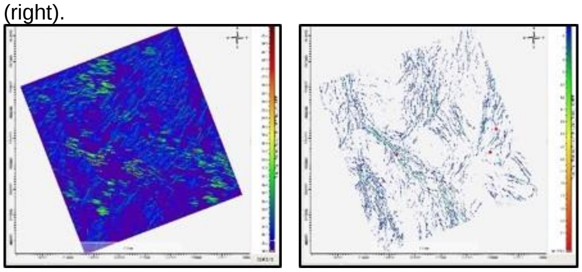

Figure 18: Area of Nearest Positive Event: Seed Vector (left), Ant-track (right).

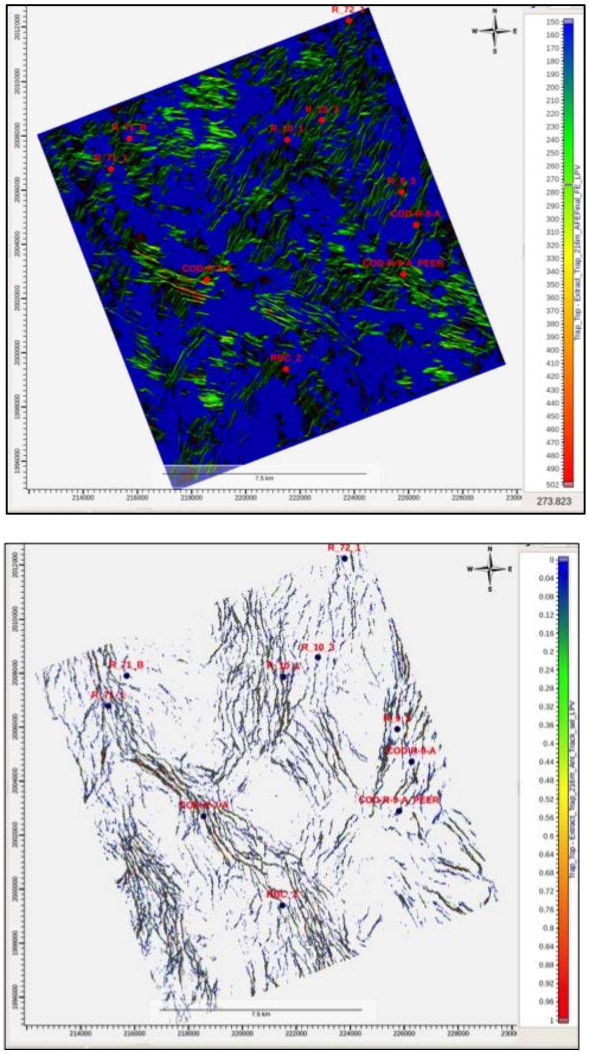

Figure 19: Merge Attributes [Largest Positive Value & Area of Nearest Positive Event]: AFE Vector (left), Ant-track (right).

Conclusions

The study demonstrates that depth domain diffraction imaging can be used to generate higher resolution fault definition than conventional reflectivity volumes or their derivative post-stack attributes, both for full azimuth and narrow azimuth seismic data acquisitions.

The Field A in South Cambay Basin produces hydrocarbons from fractured basement. To optimize field development, high resolution diffraction volume can be used to accurately characterize these fractures. In Field B area, diffraction volume and its post stack derivatives give a detailed information regarding the basement fracture network and thus guiding the proposed well locations, based on the best fracture density pods and locales where openness are expected. Diffraction imaging yields seismic attributes that have performed better compared to the coherency and curvature attributes from the conventionally processed seismic data. This new work-flow of adopting 3D Fault Extraction using diffraction volume already produces vast improvement in comparison of traditional ant-track work-flow using coherency/chaos volume derived from reflection seismic. The fracture density map produced from executing our work-flow can be used for discovery and/or continued development of the fractured basement reservoir in optimizing both new well placement and for design of well trajectories.

References

Chopra S, Marfurt K, Coherence attribute applications on seismic data in various guises-Part I, Interpretation, Aug 2018, Page T521-T529.
Ghosh, A., 2019, Understanding basement fracture architecture in Padra Field, South Cambay Basin, India, through full-azimuth imaging; The Leading Edge, April 2019, Page 262-267.
Koren, Z., and I. Ravve, 2011, Full-azimuth subsurface angle domain wavefield decomposition and imaging Part I: Directional and Reflection image gathers: Geophysics, 76, no. 1, S1-S13.
Benfield, N.R, Guise, A, Chase, D, 2016, Diffraction imaging – a tool to reduce exploration and development risk; First Break, Vol 34, March 2016, Page 57-63.

Acknowledgements

The authors sincerely thanks to ONGC, for providing data, necessary infrastructure to complete the project and permission to publish this study. The authors wish to express their gratitude for continuous support and suggestions to Shri R.K.Srivastava, Director (Exploration), Shri V.Pandey, ED-Basin Manager, WOB, Shri S.K.Sharma, ED-CGS, Shri P.R.Balak, GGM-HGS, ONGC, Mumbai. The views expressed here are exclusively those of the authors only, and they need not necessarily match with official views of ONGC